[1]Archana Gopinadhan

[2]Dr. Angeline Prasanna G

Ad-Tl: Alzheimer's Disease Prediction Using Transfer Learning

Abstract: - Although many statistical methods and machine learning algorithms have been explored in both clinical and research settings to extract these patterns from neuroimaging data, differentiating between Alzheimer's disease and healthy brain data in older adults (age > 75) has proven challenging due to highly similar patterns of brain atrophy and image intensities. Medical image analysis is just one field that has benefited from the widespread use of deep learning technologies in recent years. This research paper proposed AD prediction using transfer learning (AD-TL) methods. The MRI dataset has been normalized using the Multi-Layer Perception model (MLP) with the CNN algorithm. In order to improve images, the CLAHE (Contrast-Limited Adaptive Histogram Equalization) technique has been used. Image segmentation has been done with Watershed Image segmentation. The training has been done with the Residual network (ResNet 50) with Alex net. Finally, the classification has been done with the Deep Convolutional neural network (DCNN) algorithm. According to the experimental data, the classification accuracy of the technique provided in this study may reach 99%.

Keywords: Alzheimer's disease, Convolutional neural network, Deep Convolutional neural network, ResNet, , Prediction

1. Introduction

Alzheimer's disease (AD) is a multi-factorial, irreversible [1], degenerative neurological brain condition that gradually destroys brain cells, resulting in memory and cognitive impairment and, finally, the inability to perform even the most fundamental functions [2]. Due to the long-term effects on cognition, this condition is a leading cause of dementia [3]. This gradual decline over time is characteristic of neurodegenerative dementia [4]. Diagnosing Alzheimer's disease requires a thorough evaluation of the patient's medical history, a short mental state examination (MMSE), and physical and neurological testing. Brain morphology, functional brain activity, and alterations may also be evaluated non-invasively using structural magnetic resonance imaging (sMRI) and resting-state functional magnetic resonance imaging (rs-fMRI) [6]. Patients must lie prone on the MRI table and not move throughout structural (anatomical) and rs-fMRI scans [7]. [8-12]. This allows data collection to continue independent of the influence of a given task on functional brain activity. Alzheimer's disease shrinks the hippocampus and cerebral cortex while expanding the brain's ventricles [13]. The degree of these consequences is influenced by the stage of the disease's development. MR images of individuals with severe Alzheimer's disease show substantial hippocampal and cerebral cortical atrophy and considerable ventricular enlargement [14]. The areas and connections in the brain responsible for reasoning, remembering (particularly short-term memory), planning, and judging are all negatively impacted. Wounded areas of the brain have reduced MR image (or signal) intensities in MRI and rs-fMRI due to the death of nearby brain cells [15-17].

Nonetheless, a number of the signals identified in AD imaging data are also present in data from the general population as they age [18]. Accurate data classification demands extensive knowledge and ability when differentiating between data related to Alzheimer's disease (AD) and photos of older adults showing usual ageing indications (i.e. MMSE) [19]. Clinicians have been looking for a way to classify MR-based imaging data (including structural MRI and rs-fMRI data) and, more significantly, to separate data from patients with brain diseases from data from healthy individuals [20-22]. Researchers and doctors will be aided in their quest to find a cure for Alzheimer's by the robust machine learning algorithm known as Deep Learning, which can detect brain illness [23-24].

This paper's primary contributions are as follows:

---

[1] Research Scholar, Department of Computer Science, AJK College of Arts and Science, Coimbatore- 641 105. Email: archanagopinadhan@gmail.com

[2]Former Associate Professor and Head, Department of Computer Science, AJK College of Arts and Science Coimbatore- 641 105.

- MRI image normalization using MLP with CNN algorithm
- Image enhancement using CLAHE with histogram equalization
- Image segmentation has been done with watershed segmentation
- The dataset has been trained with RESNet50 with AlexNet architecture
- AD Multi-class classification using D-CNN algorithm.

In the second part of this study, this paper will examine the techniques now used in the diagnosis of AD. Figure 3 depicts the AD-TL model. Section 4 presents the AD-TL model's findings and discusses them. In Section 5, we present the final conclusions and provide some ideas for further study.

2. Literature Survey

A. Amrutesh et al. (2022) based on their findings, the authors recommend utilizing Transfer learning (TL) and Machine learning (ML) to analyze Magnetic resonance imaging (MRI) scans and other medical data in order to diagnose Alzheimer's disease. Brain image images and Comma Separated Values (CSV) files containing data on Alzheimer's disease were analyzed for classification purposes. It was investigated how the classification accuracy of preexisting TL and ML models varied across datasets by comparing them. Six TL models were tested using different optimizer parameters on MRI datasets with the goal of identifying Alzheimer's disease (AD). InceptionV3 (Adam as Optimizer) and the Random Forest model obtained 99.5% and 92.134% classification accuracy in the experiments, respectively, out of the various TL and ML models studied.

A. Kumar et al. (2022) The author examines how aspects like the number of visits, the number of persons, the size of the brain graph produced, and the size of the dataset affect the accuracy of Graph Convolutional Network (GCN) models for classification in rs-fMRI-obtained brain functional networks. The author conducted this analysis using information on Alzheimer's disease. The author also developed a transfer learning strategy for training models on massive datasets and then applying those models to classification problems in networks with much smaller data sets. This was crucial for analyzing various brain networks when information was limited. The author concludes by proposing HPC acceleration approaches, such as Compute Unified Device Architecture (CUDA) streams, to shorten the training period.

A.Raj et al. (2022) The author proposes a unique CNN architecture with efficientNetV2 for the diagnosis of Alzheimer's disease, based on the Change technique, which has shown good results for overall multiple photos. The suggested approach is meant to maximize the usage of in-house resources. On a subset of the Alzheimer's disease Neuroimaging Initiative (ADNI) database consisting of 4 patients, the author obtained a classification performance of 1.0 for AD/CNN and 0.95 for AD/CNN+EfficientNetV2. More work has to be done to improve the frame rate at which data can be analyzed. Modifications to the structural approach of the suggested method may cut down on the time and energy needed to construct the model computationally.

B. Tamm et al. (2023) the author share the results of these authors ADReSS-M competition entry. In addition to outperforming the best baseline model, these authors method was also highly resistant to model initialization errors. These authors unique contribution was the combination of a pre-training phase and a mixed-batch fine-tuning phase.

C. A. Ortiz Toro et al. (2021) The findings presented here suggest that some radioman features (such LAHGLE) may be useful as future biomarkers in the diagnosis of Alzheimer's disease. The hippocampus and the amygdale were shown to be the most prominent locations for MRI AD/CN distinction, which was consistent with earlier research.

M. Lavanya et al. (2018) here, a cutting-edge Deep learning (DL) model was expected to track Alzheimer's disease's development. Since the disease was thought to progress over time, the model takes this temporal information into account. The suggested model improves upon prior methods by classifying the present diagnostic status in addition to predicting future illness progression. The experimental results show that compared to other methods, these authors model performs better. Additionally, these authors method includes a table for various data sizes.

M. Mahyoub et al. (2021) The authors' stated goal was to better understand the ADNI dataset, and they made no claims about the therapeutic use of the data they compiled. The studies in this study made use of data from a subset of the Alzheimer's Disease Neuroimaging Initiative (ADNI) dataset. All respondents were anonymous, and the data retrieved included indicators of potential vulnerability to Alzheimer's disease. Lifestyle, demographics, and personal qualities were examples of behavioral risk factors, whereas medical history, genetics, and the presence or absence of symptoms was examples of biological risk factors.

3. Materials and Methods

The proposed model is named the AD-TL method for early AD prediction. This AD-TL method has utilized MLP for noise removal, and hybrid deep learning algorithm for training, and CNN for classification.
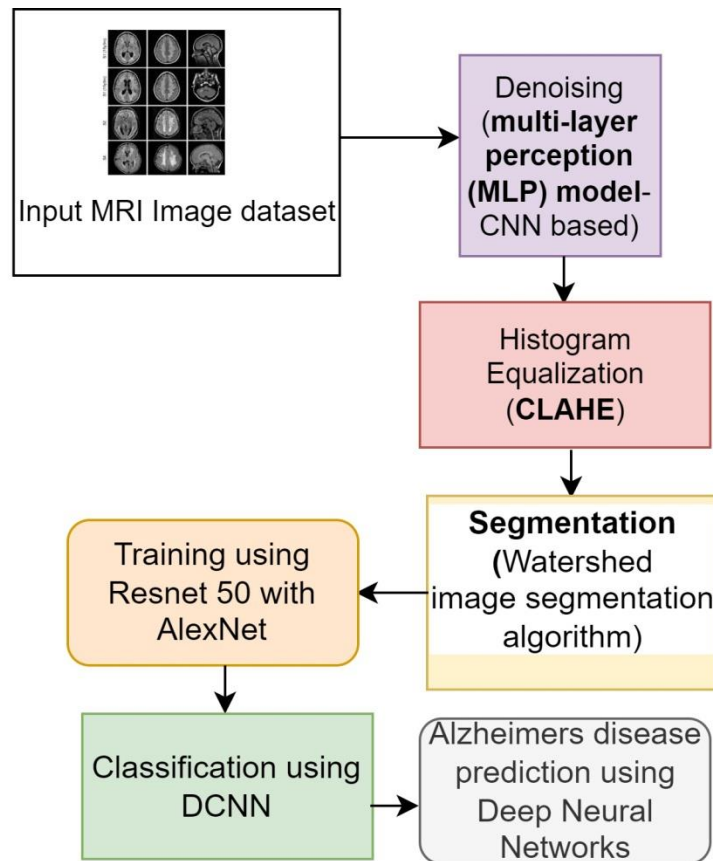

Figure 1: Architecture Diagram for AD-TL framework

3.1 Dataset Description:

The MR imageon this page may be used to build a diagram of the brain's architecture, including the medulla oblongata, emphasizinginput structure. Many parts of a picture may be identified individually. The proposed work is executed on AD-related datasets obtained from the https://www.kaggle.com/datasets/tourist55/alzheimers-dataset-4-class-of-images website link.
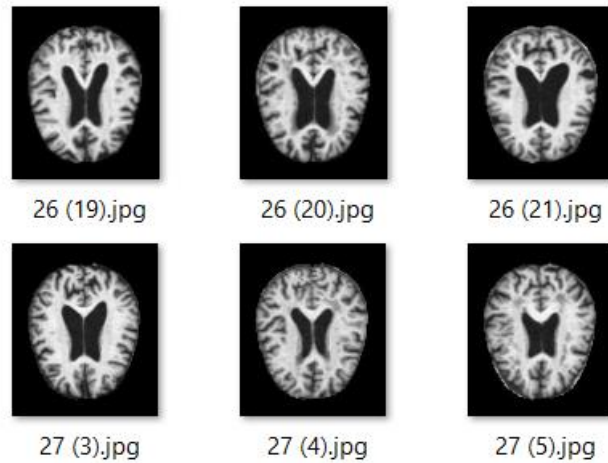
Figure 2: Sample MRI Images

3.2 Denoising using Multi-Layer Perception Networks With CNN

After dataset collection, denoising using Multi-Layer Perception (MLP) Networks with Convolutional Neural Networks (CNN) entails utilizing a CNN to extract meaningful spatial features from the noisy input data, such as noisy images, followed by one or more MLP layers that learn to map these noisy representations to cleaner versions.

Denoising using Multi-Layer Perception (MLP) Networks with Convolutional Neural Networks (CNN) is a data processing technique that leverages the strengths of both CNNs and MLPs to remove noise from noisy data L. Zhang (2023). This method typically involves the use of a CNN for feature extraction, followed by one or more MLP layers for noise reduction, trained on a dataset containing pairs of noisy and clean data. The CNN extracts relevant features, while the MLPs learn to map noisy representations to cleaner versions, ultimately producing denoised output. This approach has broad applications in image and signal processing, ensuring noise reduction while preserving essential information in the data.

Figure 2 depicts the components of a multi-layer perceptual architecture, which includes two "hidden" layers in the middle and a "output" layer at the end. A network of this kind consists of three layers: an input layer, a layer containing several computer nodes, and an output layer. The initial signal grows radically as a byproduct.

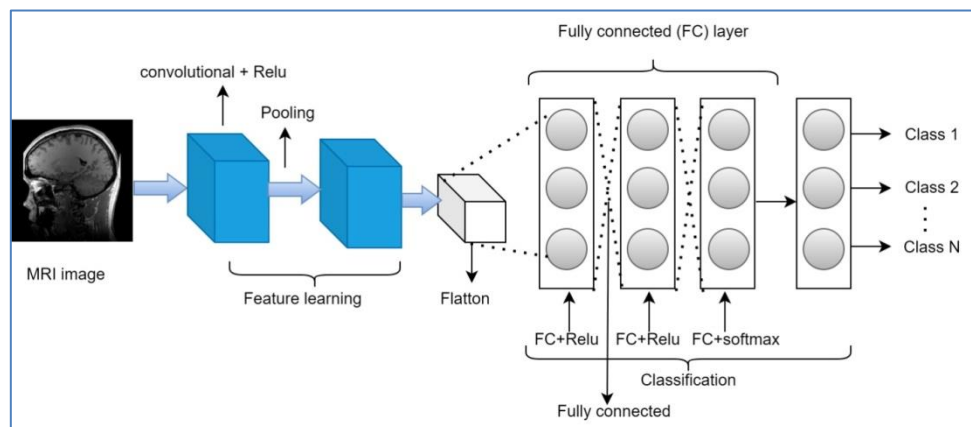Using the back-propagation algorithm, multi-layer perception networks are trained for networkanalysis.

Figure 3: Multi-Layer Perception Schematic with Two Secret Layers

(1) Objective function Selection

The regularisation part of the network is driven by design, i.e. Bayes methods are led in neural network analysis. Assuming weight follows a Gaussian distribution, the regularisation item appears as follows:

$$R(w) = \frac{1}{2}\sum_{j=1}^{N_w} w_j^2 \qquad \text{------ (1)}$$

Crossover tests are utilized for training the network in the network training progression. After the allotted number of cycles, check the samples. Let's pretend that C (w) is a performance function, the mean square training error is $E_T(w)$, and the formula for C (w) is as follows (2):

$$C(w) = E_T(w) + \xi R(w) \qquad \text{-------- (2)}$$

ξ is regularising parameter.

Consider the case when the generalization error, denoted by $E_G(w)$, is larger than the global error, denoted by $E(w)$, as indicated by the following formula (3):

$$E(w) = \frac{C(w)+E_G(w)}{2} \qquad \text{------- (3)}$$

The goal of this optimization problem is to find the minimum value of the sufficiency function, given by the formula (4):

$$f(w) = \frac{1}{1+E(w)} \qquad \text{------- (4)}$$

Algorithm 1: Multi-Layer Perception Networks With CNN

Input:
- Initial weights $w_{initial}$
- Regularization parameter ξ

Step:
1. Initialize the weights w = $w_{initial}$.
2. For each iteration:
a. Perform a forward pass through the neural network to compute $E_T(w)$ on the training data.
 b. Compute $R(w)$ using the regularization term.
c. Calculate $C(w) = E_T(w) + \xi R(\text{w})$.
d. Calculate the generalization error $E_G(\boldsymbol{w})$.
e. Compute $E(w) = \frac{C(w)+E_G(w)}{2}$.
f. Update the weights using the chosen optimization method to minimize $E(w)$.
3. Repeat the above steps until a stopping criterion is met (e.g., a maximum number of iterations or convergence criteria).

Output:
- Optimized weights w that minimize $E(\text{w})$.

3.3 Histogram equalization using Contrast Limited Adaptive Histogram Equalization

Contrast Limited Adaptive Histogram Equalization (CLAHE) is an image enhancement technique applied after denoising to improve contrast and visual quality P. M. Ebin and P. Ranjana (2022). CLAHE is adaptive, dividing images into tiles and equalizing histograms locally to preserve fine details and avoid noise amplification. By limiting contrast enhancement and using interpolation to smooth transitions between tiles, CLAHE ensures a natural appearance.

It has been shown that Contrast Limited Adaptive Histogram Equalization (CLAHE) is superior to Adaptive Histogram Equalization (AHE). CLAHE mitigates the problems caused by AHE by restricting the improvement of contrast in uniform regions. Assigning additional pixels to the same grayscale range, as shown in a histogram peak that depends on context.

To do this, CLAHE adjusts the intensity values in the image, working in tiny squares (called tiles) and using bilinear interpolation to eliminate the edges of the tile and smooth out the neighbouring pixels. Conventional histogram equalization may lead to brightness saturation. However, CLAHE considerably decreases picture noise.

In this scenario, the exponential distribution will be used to spread the grey-level distribution among the pixels in the histogram, which recognizes that the pixels may have different distributions.

$$\beta = \frac{M}{N}\left(1 + \frac{a}{100}(S_{max} - 1)\right) \qquad \text{------ (5)}$$

Exponential:

$$g = g_{min-(1/\alpha)*}ln[1 - p(f)] \qquad \text{------ (6)}$$

g_{min}= minimum pixel value

g_{max} = maximum pixel value

g = computed pixel value

α = parameter

$p(f)$ = cpd (Cumulative probability distribution)

3.4 Segmentation using Watershed image segmentation

Utilizing the Watershed Image Segmentation method after Histogram Equalization involves enhancing image contrast through Histogram Equalization, making objects and boundaries more distinct Y. He et al. (2023). Watershed segmentation, inspired by topographic water flow, then partitions the image into regions or objects based on the gradient information in the image, using markers placed at regions of interest.

The kernel density estimation method, commonly known as the Parzen window technique in pattern recognition, is widely used to calculate density estimates in feature space analysis. The multivariate fixed bandwidth kernel density estimate is denoted as where n is the number of data points and d is the dimension of the space in which they are located.

$$f^\Lambda(x) = \frac{1}{nh^d}\sum_{i=1}^{n} K(\frac{(x-x_{i)}}{h} \qquad \text{-------- (7)}$$

Where h is the constant bandwidth across the network. $x \in R^d$ And k(x)is a radically symmetric kernel

Identifying its modes is the first step in evaluating a feature space where f(x) represents the underlying density. The modes are positioned among the gradient's zeros $\nabla f(x)0$. The mean-shift strategy is the most effective method for locating these zeros without estimating the density. The mean shiftvector always points in the direction of the most significant density increase.

Consider the classification of z into C classes, Z_i i=1…C. Let m_i represent the average of the N_i data points in classz_i

$$m_i = \frac{1}{N_i}\sum_{z\in Z} z \qquad \text{-------- (8)}$$

$$Let\ S_{T=\sum_{z\in Z}\|z-m\|}2\ and\ S_w = \sum_{i=1}^{c} S_i = \sum_{i=1}^{c}\sum_{z\in z_i}\|z - m_i\| \qquad \text{---------- (9)}$$

The definition of the dimension J is

$$J = \frac{(S_T - S_W)}{s_W} \qquad \text{------- (10)}$$

It compares the distances between members of distinct classes $(S_{T-}S_W)$ against those between members of the same class S_W. A more excellent value of J indicates that the classes are more apart, but the members within each class are closer together, and vice contrarily.

Algorithm 2: Watershed image segmentation
Input:
A dataset with data points, where each data point has a feature vector x and is associated with a class label Z_i
Step:
• For each class Z_i (i = 1...C), compute the average m_i of the data points in that class using:
$m_i = \frac{1}{N_i}\sum_{z\in Z}z$
• Calculate the total scatter S_T, which measures the sum of squared distances between all data points and their class means using:
$Let\ S_{T=\sum_{z\epsilon Z}\|z-m\|}2\ and\ S_w = \sum_{i=1}^{c}S_i = \sum_{i=1}^{c}\sum_{z\in z_i}\|z-m_i\|$
• Use the defined metric J in to evaluate the separation between classes. A higher J value indicates better class separation, where classes are more apart, but data points within each class are closer together.
$J = \frac{(S_T - S_W)}{S_W}$
Output:
The modes of the density estimate (identified peaks)

3.5 Training using ResNet-50 with AlexNet

ResNets is a design for neural networks that incorporates the Residual Learning method into its wiring B. N. Esi Nyarko et al. (2022). This approach prevents parameter values from being saturated by adding the Value of the shortcut, which is the single layer of the liner player linked to the network from input to output after it passes through one or more specified layers and the function F(x) (vanishing gradient).

On the assumption that a complex function may approximate the output of several nonlinear layers, Residual Learning theory draws the conclusion that such a mapping exists. Means $F(x) = H(x) - x$, it can convert the formula to $H(x) = F(x) + x$, training can be accelerated and vanishing gradients avoided if we create a shortcut using x as an input to the function F(x).

To combat the vanishing gradients, ResNets made use of shortcut connections to skip over one or more levels, creating a structure known as a Residual Block. ResNets must create two separate Residual Blocks, the identity block and the convolutional block. The identifying Block of ResNets is a typical Residual Block with identical input and output sizes. By use of Residual Learning, Identity Block demonstrated Eq (11).

$$\mathcal{Y} = F(x,\{W_i\}) + x \qquad\qquad \text{-------- (11)}$$

The Identity Block is shown in its original state in Figure 4. The ReLU function acts as a switch, switching the model to its nonlinear, formula-described state. Y=max (0, x) (0, x). A Convolutional Layer, the Weight Layer, and the subsequent Batch Normalization technique are used to standardize features in a zero-mean condition by a factor of 1.
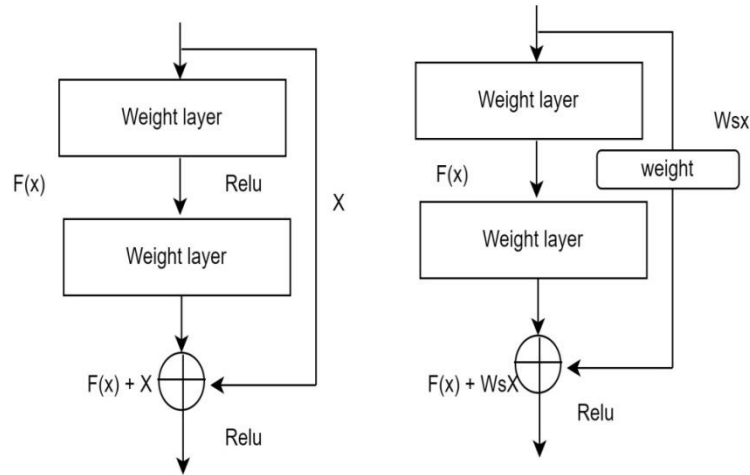
Figure 4: Original Identity Block and Convolutional Block structure.

Like the Identity Block, the Residual Block, known as the Convolutional Block, uses the Residual learning technique. In contrast, the quick cut built a Weight Layer to adjust the Value of the specified parameterW_s. The layout is shown in Fig. 5, and the Convolutional Block's universal formula is represented by the (12).

$$\mathcal{Y} = F(x, \{W_i\}) + W_s x \qquad \text{-------- (12)}$$

As shown in this study, reduced training times were achieved by adding a weight layer to the Identity Block and Convolutional Block model. Figure 5 depicts Identity Block and Convolutional Block variants.
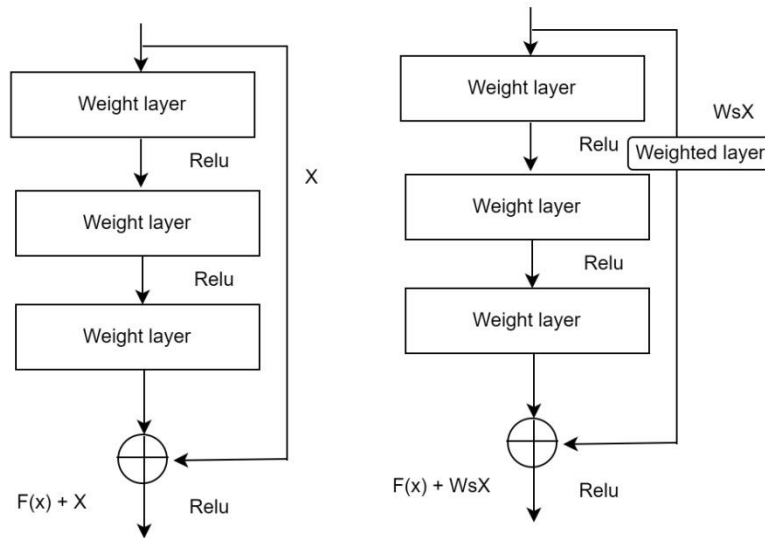

Figure 5: Variable Identity Block and Convolutional Block structure.

The convolutional 7x7 input layer of the ResNet-50 model is shown in Figure 5. Convolutional blocks and converted identity blocks, each with three convolution layers and a shortcut link, comprise the sixteen residual blocks divided over stages 2-4-5. One convolutional block and two identity blocks, each with a block size of 64, make up Stage 2. Stage 3 block size includes one convolutional block and three identity blocks for 128. This stage's neural network consists of 1 convolutional block and 5 identity blocks, with a block size of 256. In the fifth stage, we use a 512-by-512 block size for both the convolutional and identification blocks. To adapt the feature size to the parameters of each stage, the convolutional block is placed at the start of each phase.
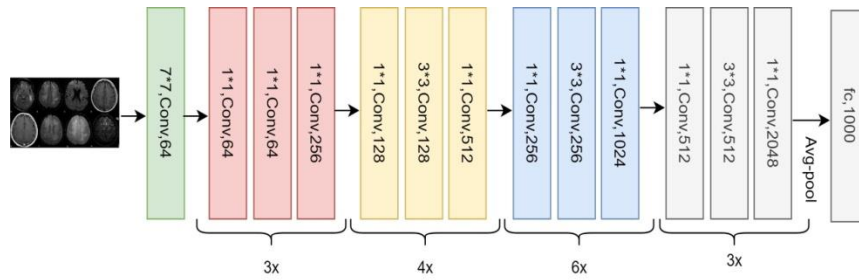
Figure 6: Structure of the ResNet-50 A-disease recognition model.

3.5.1 Description of AlexNet

AlexNet is a well-known design for neural networks. It received widespread recognition for participating in and winning the 2012 ImageNet Large Scale Visual Recognition Challenge. The network achieves a phenomenal error rate of 15.3%, 10.8 percentage points lower than its closest competitor. AlexNet is based on the principle that model depth is crucial for performance. Therefore, it was coded in CUDA to be executed on a GPU for faster training. AlexNet is not the first network to train on GPU, but its impact in this sector is enormous. One of the most influential works in image recognition, it stimulates more research than GPU training. The standard AlexNet (Figure 5) consists of five convolutional layers, three max-pooling, and three fully linked layers.
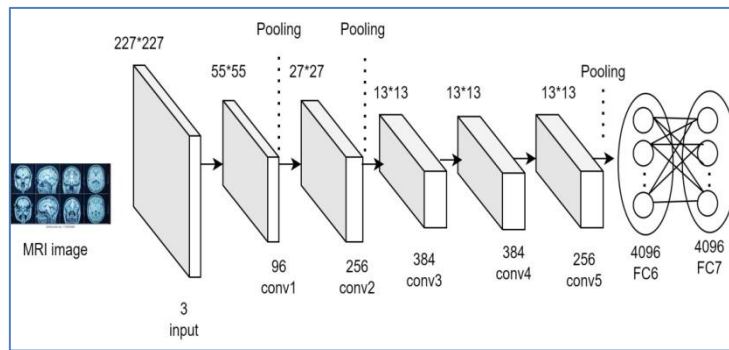

Figure 7: Alexnet architecture

3.6 AD Prediction using Deep Convolutional neural network Model

An advanced use of deep learning in medical imaging is the prediction of Alzheimer's disease (AD) using a Deep Convolutional Neural Network (CNN) model. Gathering and preprocessing of magnetic resonance imaging (MRI) images of the brain is the first step in creating convolutional neural network (CNN) architecture with convolutional and pooling layers for feature extraction and categorization. To learn to tell healthy and AD-affected brains apart, this model is trained on a labelled dataset. Metrics evaluate how well the model can make AD predictions in terms of accuracy, sensitivity, and specificity. After validation, the trained model is deployed for real-world use, offering the potential for early AD diagnosis and monitoring by analyzing new MRI scans. Refinement and optimization techniques may be applied to enhance the model's performance further, contributing to more effective AD management and treatment.

Convolutional layers are the backbone of every deep CNN, and advanced activation functions allow them to perform at their peak. The suggested deep CNN (deep ConvNet) model uses a deep convolutional neural network to automatically extract data from whole-brain MRI scans for Alzheimer's disease detection. As shown in Fig. 2, the proposed model requires sliced, preprocessed 2D data as input. Each book has 500–600 individual slices, depending on the subject.

With the same padding and image size of 300 300 1, we used six blocks of replicated 2D convolutional layers. All convolutional layers had the same kernel size. Still, filters ranging from 4 to 128 pixels in size were employed to extract complex and multi-scale information, creating a feature map from which these characteristics could be sent to other layers and utilized to extract more complicated features.

The filters that make up a CNN's architecture are responsible for learning different aspects of an image: initially, its edges, then its complicated forms, and last, its colours and finer details. CNN design caters for the computational capacity of the input layer by lowering the dimensionality of the input form via max pooling. Additionally, the sizes of each convolutional layer's filter change.

Algorithm 3: Deep Convolutional neural network
Input:
Whole-brain MRI scans, pre-processed into 2D slices, are provided as input to the CNN model. Each scan typically consists of 500-600 individual slices
Step:
•   Design a deep Convolutional Neural Network (CNN) model with multiple convolutional layers. Each layer performs feature extraction and abstraction from the input data.
•   Configure the convolutional layers to have filters of varying sizes, ranging from 4 to 128 pixels. This diversity in filter sizes helps the model extract complex and multi-scale features from the MRI scans.
Output:
The output of the algorithm is a deep Convolutional Neural Network (CNN) model that has learned to automatically extract relevant features from whole-brain MRI scans for Alzheimer's disease detection.

4. Experimental Results and Discussion

The recommended model was developed in Python (version 3.8). In this chapter, we provide the outcomes of our experiments. ResNet50 and Alexnet, both deep neural networks, have been utilized for both training and testing purposes. Table 1 displays our trained and tested model's findings.
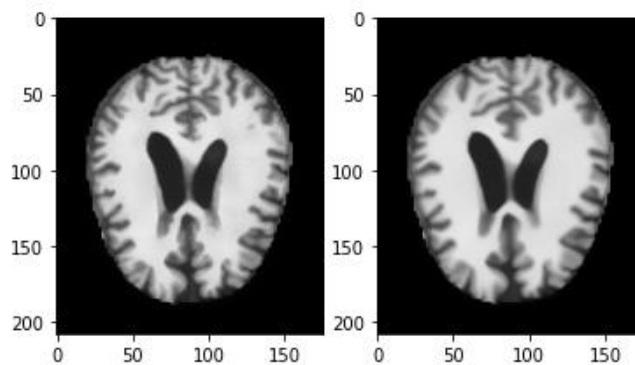
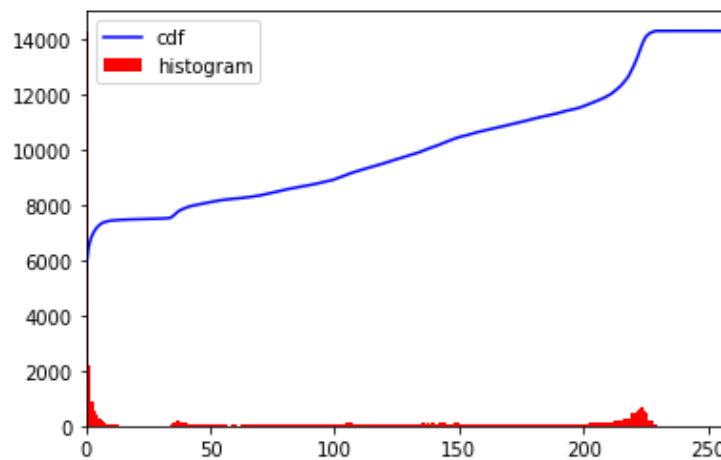Figure 8: Image Noise Removal using MLP with CNN

Figure 9: Histogram equalization using the CDF function

The MRI images are noise removed using MLP Algorithm, and the results are illustrated in figure 8. And the histogram equalization done with Cumulative Density Function (CDF) is represented in figure 9.
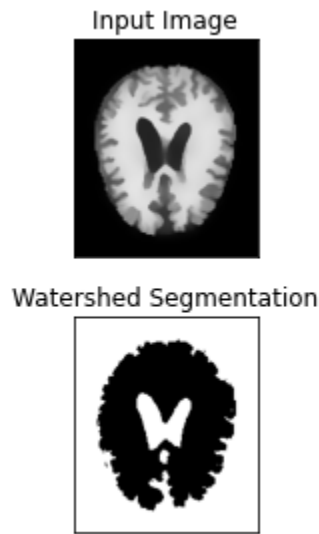

Figure 10: Image Segmentation

Table 1: Training and evaluating values based on the 10 Epoch

| Epoch	Training Loss	Validation Loss	Training Accuracy	Testing Accuracy
1	00.1538	00.0637	00.9545	00.9799
2	00.0550	00.0479	00.9830	00.9834
3	00.0354	: 0.0459	00.9894	00.9837
4	00.0248	00.0440	00.9919	00.9871
5	00.0167	00.0478	00.9944	00.9857
6	00.0121	00.0523	00.9957	00.9853
7	00.0080	00.0550	00.9974	00.9857
8	00.0071	00.0567	00.9977	00.9855
9	00.0051	00.0486	00.9983	00.9869
10	00.0066	00.0617	00.9977	00.9853
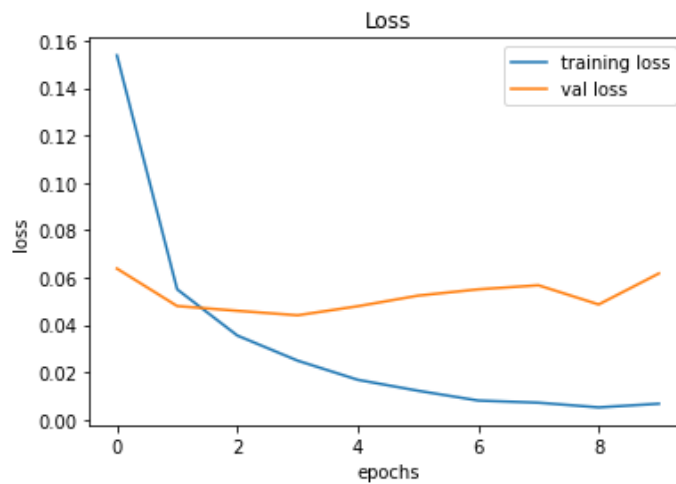
Figure11: Training and testing loss

As illustrated in Figure 11, the suggested model is trained using loss values. The X-axis represents the Epoch, and the Y-axis represents the lost Value.
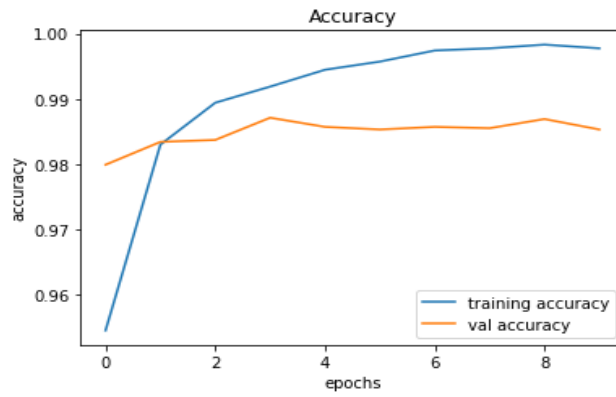
Fig 12: Training and testing Accuracy.

The CNN-ResNet has been trained using 10 Training Epochs, and Figure 12 displays the testing accuracy. The Y-axis reflects the accuracy, while the X-axis represents the Epoch number.
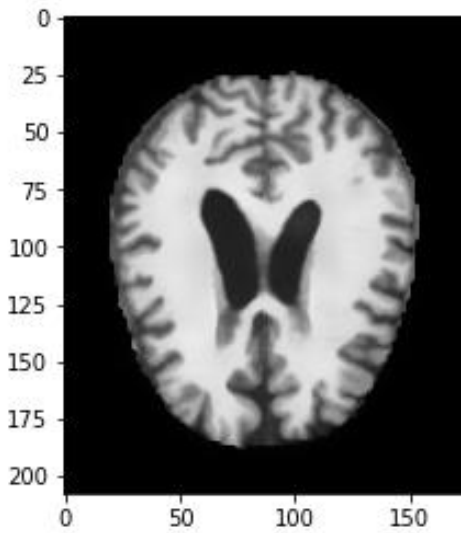

Figure 13: Input MRI Image will be predicted by Moderate Demented

The input MRI image predicted using the proposed model with Moderate Demented output is shown in figure 13.
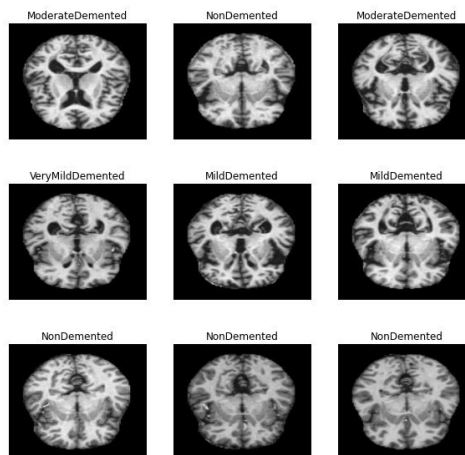

Figure 14: CNN Image Classification

The proposed model achieves 98% accuracy. And the CNN has classified the MRI image as multi-class classification,as shown in figure 14.
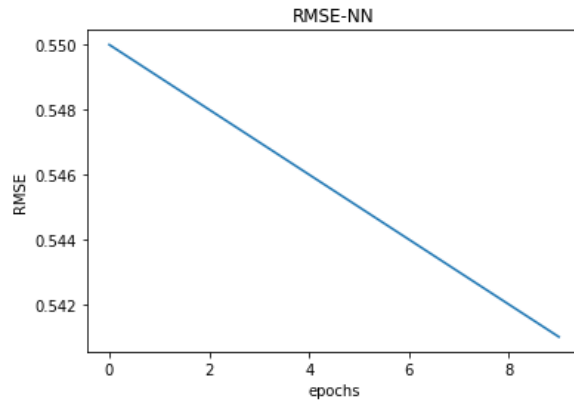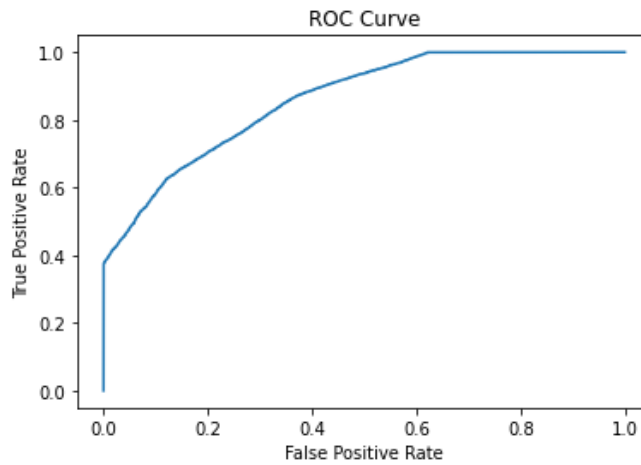

Figure 15: RMSE Value

Figure 16: ROC Curve

The prediction overall confusion matrix is shown in figure 15. The RMSE Value is represented in figure 16. The ROC curve is represented in figure 17.

Table 2: Performance metrics comparison table

	Algorithm	Accuracy (%)	Precision	Recall	F-measure
Existing authors	A. Amrutesh et al. [1]	92.13%	91.01%	90.21%	92.11%
	A. B. Rabeh et al. [2]	94.44%	93.65%	94.00%	95.31%
	A. Yashodhar and S. Kini [4]	92.20%	91.17%	94.23%	91.21%
Existing methods	CNN	95.21%	96.32%	94.54%	95.87%
	DNN	96.11%	95.41%	95.61%	94.23%
	RCNN	97.54%	97.89%	98.21%	98.61%
Proposed methods	DCNN	98.99%	99.11%	99.31%	98.71%

The table 2 shows the evaluation of Alzheimer's disease prediction algorithms; the provided results indicate the performance metrics of various existing and proposed methods. Existing approaches, led by authors 1, 2, and 4, demonstrated commendable accuracy ranging from 92.13% to 94.44%, with associated precision, recall, and F-measure values showing the robustness of their models. Among these, the RCNN method achieved the highest accuracy of 97.54% and excelled in precision, recall, and F-measure metrics, surpassing existing CNN and DNN models. However, the proposed DCNN method outperformed all previous techniques, boasting an impressive accuracy of 98.99% and exhibiting exceptionally high precision, recall, and F-measure values, indicating its potential as a highly effective tool for Alzheimer's disease prediction. These results signify substantial advancements in the field, particularly with the introduction of the DCNN model, which holds promise for enhanced diagnostic accuracy in Alzheimer's disease detection.
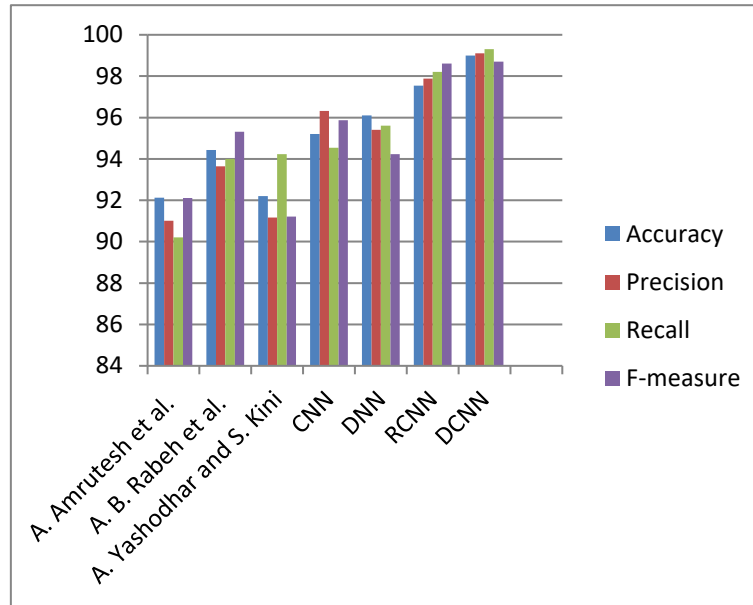

Figure 17: Performance metrics comparison chart

The figure 17 shows performance metrics comparison chart the x axis shows methods and the y axis shows values in percentage.

5. Conclusion

This study reported on detecting Alzheimer's disease (AD) using a deep learning model, which assists clinicians in the diagnostic process. This research paper has proposed an AD-TL framework for predicting AD as early as. Vascular enlargement and brain atrophy Image segmentation are used to identify more giant Vascular/tumours. The degree of enlargement defines whether a patient is healthy, in the initial stage of Alzheimer's, in the second stage of Alzheimer's, or has moderate cognitive impairment. Brain shrinkage is another crucial element of Alzheimer's disease diagnosis. This research presented a paradigm for the identification of AD at an early stage. The MRI Image noises wereremoved using MLP with CNN, and the image segmentation was done with watershed image segmentation. The training has been done with Resnet50 with Alexnet architecture. The classification has been done with DCNN. The research reveals that the use of improves classification accuracy. This solves the challenge of early detection while causing no brain injury, and the proposed approach achieves 98.99% accuracy. This will help to advance medical imaging studies—the future scope of this study is to enhance the authentic MRI images to integrate mobile applications.

Reference

[1]   A. Amrutesh, G. B. C G, A. A, A. R. KP and G. S, "Alzheimer's Disease Prediction using Machine Learning and Transfer Learning Models," 2022 6th International Conference on Computation System and Information Technology for Sustainable Solutions (CSITSS), Bangalore, India, 2022, pp. 1-6, doi: 10.1109/CSITSS57437.2022.10026365.

[2]   A. B. Rabeh, F. Benzarti and H. Amiri, "CNN-SVM for prediction Alzheimer disease in early step," 2023 International Conference on Control, Automation and Diagnosis (ICCAD), Rome, Italy, 2023, pp. 1-6, doi: 10.1109/ICCAD57653.2023.10152440.

[3]   A. Kumar, V. Balaji, M. A. Chandrashekar, A. Dukkipati and S. Vadhiyar, "Graph Convolutional Neural Networks for Alzheimer's Classification with Transfer Learning and HPC Methods," 2022 IEEE International Parallel and Distributed Processing Symposium Workshops (IPDPSW), Lyon, France, 2022, pp. 186-195, doi: 10.1109/IPDPSW55747.2022.00043.

[4]   A. Yashodhar and S. Kini, "Comparison of Transfer Learning algorithm in predicting Alzheimer's disease," 2023 International Conference on Advances in Electronics, Communication, Computing and Intelligent Information Systems (ICAECIS), Bangalore, India, 2023, pp. 183-187, doi: 10.1109/ICAECIS58353.2023.10170318.

[5]   A.Raj, S. Bujare, A. Gorthi, J. Malik, A. Das and A. Kumar, "Alzheimer's Disease Recognition using CNN Model with EfficientNetV2," 2022 2nd Asian Conference on Innovation in Technology (ASIANCON), 2022, pp. 1-5, doi: 10.1109/ASIANCON55314.2022.9908834.

[6]   Andersen, E., Casteigne, B., Chapman, W. D., Creed, A., Foster, F., Lapins, A., … Sawyer, R. P. (2021). Diagnostic biomarkers in Alzheimer's disease. Biomarkers in Neuropsychiatry, 5, 100041. doi:10.1016/j.bionps.2021.100041

[7]   B. Tamm, R. Vandenberghe and H. Van Hamme, "Cross-Lingual Transfer Learning for Alzheimer's Detection from Spontaneous Speech," ICASSP 2023 - 2023 IEEE International Conference on Acoustics, Speech and Signal Processing (ICASSP), Rhodes Island, Greece, 2023, pp. 1-2, doi: 10.1109/ICASSP49357.2023.10096770.

[8]   B. N. Esi Nyarko, W. Bin, J. Zhou, G. K. Agordzo, J. Odoom and E. Koukoyi, "Comparative Analysis of AlexNet, Resnet-50, and Inception-V3 Models on Masked Face Recognition," 2022 IEEE World AI IoT Congress (AIIoT), Seattle, WA, USA, 2022, pp. 337-343, doi: 10.1109/AIIoT54504.2022.9817327.

[9]   C. A. Ortiz Toro, N. Gutiérrez Sánchez, C. Gonzalo-Martín, R. Garrido García, A. Rodriguez González and E. Menasalvas Ruiz, "Radiomics Textural Features Extracted from Subcortical Structures of Grey Matter Probability for Alzheimer's Disease Detection," 2019 IEEE 32nd International Symposium on Computer-Based Medical Systems (CBMS), 2019, pp. 391-397, doi: 10.1109/CBMS.2019.00084.

[10] Haussmann, R., Noppes, F., Brandt, M. D., Bauer, M., & Donix, M. (2021). Lithium: A therapeutic option in Alzheimer's disease and its prodromal stages? Neuroscience Letters, 760, 136044. doi:10.1016/j.neulet.2021.136044

[11] K. T. -I. Ong et al., "Evidence-Empowered Transfer Learning for Alzheimer's Disease," 2023 IEEE 20th International Symposium on Biomedical Imaging (ISBI), Cartagena, Colombia, 2023, pp. 1-5, doi: 10.1109/ISBI53787.2023.10230842.

[12] L. Zhang, "LMLP-DPDRSD: Leveraging Multi-Layer Perception for Diagnosing Parkinson's Disease Recognition from Sound Dataset," 2023 4th International Conference on Electronic Communication and Artificial Intelligence (ICECAI), Guangzhou, China, 2023, pp. 119-123, doi: 10.1109/ICECAI58670.2023.10176519.

[13] M. Lavanya, R. R. Chandan, P. Rajasekar, P. R. Rham, M. Deivakani and A. S. Mahesh Kumar, "Machine Learning-based Alzheimer's Disease Prediction using Personalized Methods," 2022 3rd International Conference on Smart Electronics and Communication (ICOSEC), Trichy, India, 2022, pp. 1278-1283, doi: 10.1109/ICOSEC54921.2022.9952018.

[14] M. Liu, M. Y. Shalaginov, R. Liao and T. H. Zeng, "A Deep Convolutional Neural Network For Early Diagnosis of Alzheimer's Disease," 2022 IEEE-EMBS Conference on Biomedical Engineering and Sciences (IECBES), Kuala Lumpur, Malaysia, 2022, pp. 58-61, doi: 10.1109/IECBES54088.2022.10079301.

[15] M. Mahyoub, M. Randles, T. Baker and P. Yang, "Comparison Analysis of Machine Learning Algorithms to Rank Alzheimer's Disease Risk Factors by Importance," 2018 11th International Conference on Developments in eSystems Engineering (DeSE), 2018, pp. 1-11, doi: 10.1109/DeSE.2018.00008.

[16] N. A. Vats, P. Barche, G. S. Mirishkar and A. K. Vuppala, "Exploring High Spectro-Temporal Resolution for Alzheimer's Dementia Detection," 2022 IEEE International Conference on Signal Processing and Communications (SPCOM), 2022, pp. 1-5, doi: 10.1109/SPCOM55316.2022.9840847.

[17] P. M. Ebin and P. Ranjana, "A Variant Binary Classification Model for No-DR Mild-DR Detection using CLAHE Images With Transfer Learning," 2022 International Conference on Computing, Communication, Security and Intelligent Systems (IC3SIS), Kochi, India, 2022, pp. 1-5, doi: 10.1109/IC3SIS54991.2022.9885665.

[18] Rapaka, D., Bitra, V. R., Challa, S. R., & Adiukwu, P. C. (2021). Potentiation of microglial endocannabinoid signalling alleviates neuroinflammation in Alzheimer's disease. Neuropeptides, 90, 102196. doi:10.1016/j.npep.2021.102196

[19] S. Dixit, A. Gaikwad, V. Vyas, M. Shindikar and K. Kamble, "United Neurological study of disorders: Alzheimer's disease, Parkinson's disease detection, Anxiety detection, and Stress detection using various Machine learning Algorithms," 2022 International Conference on Signal and Information Processing (IConSIP), Pune, India, 2022, pp. 1-6, doi: 10.1109/IConSIP49665.2022.10007434.

[20] S. Hlawa and N. B. Romdhane, "Deep learning-based Alzheimer's disease prediction for smart health system," The 3rd International Conference on Distributed Sensing and Intelligent Systems (ICDSIS 2022), Hybrid Conference, Sharjah, United Arab Emirates, 2022, pp. 128-137, doi: 10.1049/icp.2022.2427.

[21] S. Y. Salunkhe and M. S. Chavan, "Prediction of Alzheimer's disease using Machine Learning Algorithm," 2022 Joint International Conference on Digital Arts, Media and Technology with ECTI Northern Section Conference on Electrical, Electronics, Computer and Telecommunications Engineering (ECTI DAMT & NCON), Chiang Rai, Thailand, 2022, pp. 400-405, doi: 10.1109/ECTIDAMTNCON53731.2022.9720362.

[22] Teipel, S. J., Dyrba, M., Chiesa, P. A., Sakr, F., Jelistratova, I., Lista, S., … Grothe, M. J. (2020). In vivo staging of regional amyloid deposition predicts functional conversion in the preclinical and prodromal phases of Alzheimer's disease. Neurobiology of Aging, 93, 98–108. doi:10.1016/j.neurobiolaging.2020.03.011

[23] Wei, X., Du, P., & Zhao, Z. (2021). Impacts of DNA methylation on Tau protein-related genes in the brains of patients with Alzheimer's disease. Neuroscience Letters, 763, 136196. doi:10.1016/j.neulet.2021.136196

[24] Y. He, S. Wang and X. Gao, "Analysis and Research of Spinal CT Image Segmentation Based on Improved Watershed Algorithm," 2023 IEEE 3rd International Conference on Electronic Communications, Internet of Things and Big Data (ICEIB), Taichung, Taiwan, 2023, pp. 119-123, doi: 10.1109/ICEIB57887.2023.10170668.